Preparing cold atomic samples in different density regimes for Rydberg studies

2015 J. Phys.: Conf. Ser. 605 012038

(http://iopscience.iop.org/1742-6596/605/1/012038)

Preparing cold atomic samples in different density regimes for Rydberg studies

M M Valado[1,2], M D Hoogerland[4], C Simonelli[2], E Arimondo[1,2,3], D Ciampini[1,2,3], O Morsch[1,2]

[1] INO-CNR, Via G. Moruzzi 1, 56124 Pisa, Italy
[2] Dipartimento di Fisica E. Fermi, Università di Pisa, Largo Pontecorvo 3, 56127 Pisa, Italy
[3] CNISM UdR Pisa, Dipartimento di Fisica E. Fermi, Università di Pisa, Largo Pontecorvo 3, 56127 Pisa, Italy
[4] Department of Physics, University of Auckland, Private Bag 92019, Auckland, New Zealand

E-mail: `valado@df.unipi.it`

Abstract. Here we present two different experimental techniques to generate atomic clouds in different density regimes that could be used as a tool to study Rydberg systems in different scenarios. As an example, we discuss an experiment in which the dynamics of Rydberg excitations were studied both in the few atom regime and in the high density regime.

1. Introduction

Rydberg excitations in ultra-cold gases have been studied extensively in the past years [1–6]. Strongly interacting Rydberg systems offer the possibility to study different problems like many-body collective effects [7, 8], or glassy features that Rydberg systems exhibit in the incoherent regime [9]. A systematic study of these effects can be done, e.g., by varying the density of the atomic sample. Here we describe two different experimental techniques which allow us to work in different density regimes, from the few atom regime, with typically $N \leq 10$ atoms, to the high density regime.

2. Experimental techniques

Our experiments are performed on magneto-optical traps (MOT) of ultra-cold 87-Rb atoms. The MOT parameters (size of the MOT beams, loading flux from a primary two-dimensional MOT, magnetic field gradient) are chosen such as to obtain clouds of sizes ranging from: $\sigma_{x,y,z} \approx 30\,\mu$m to $150\,\mu$m, containing up to $N \approx 10^5$ atoms.

In order to excite atoms to the Rydberg state we use a coherent two-step excitation scheme with a 421 nm laser beam detuned by a range from $\Delta = +500\,$MHz to $\Delta = +720\,$MHz in order to avoid population of the intermediate state. A 1013 nm laser allows us to reach Rydberg states with principal quantum numbers ranging from $n = 55$ to $n = 120$. Depending on Δ, the effective two-photon Rabi frequencies range from $\Omega = 240\,$kHz to $\Omega = 1.2\,$MHz. The waists of the beams are focused to $40\,\mu$m and $110\,\mu$m respectively. After the excitation pulse of duration between 0.2 and $100\,\mu$s, an electric field is applied for $2\,\mu$s in order to field ionize the Rydberg atoms and to accelerate the resulting ions towards a channeltron. The counting distributions are obtained by performing 200 repetitions of the experiments. The overall detection efficiency

is $\eta \approx 50\%$. During the excitation and detection sequence the MOT beams are switched off. We are also able to directly photoionize atoms [10]. To do so, the MOT beams remain switched on thus exciting atoms to the $5P_{3/2}$-level. The excited atoms are then photoionized with a $1-2\,\mu$s pulse of 421 nm laser light. The ions produced are detected using the same electric field pulses as in the Rydberg detection. We checked that the number of ions created is proportional to the number of atoms in the cloud [11]. Hence can be used to estimate N in conditions where a direct measurement using our CCD camera is not possible.

In order to vary the density of the atomic cloud by several orders of magnitude we use two different techniques.

The first technique consists in depumping some of the atoms of the sample into a hyperfine level of the ground state not coupled to the Rydberg transition. This is achieved by illuminating the atomic cloud with a short pulse of laser light of intensity $I = 3.6 \cdot I_{sat}$ (where I_{sat} is the saturation intensity of the transition $|5S_{1/2}\rangle \rightarrow |5P_{3/2}\rangle$ transition), resonant with the transition $|5S_{1/2}; F = 2\rangle \rightarrow |5P_{3/2}; F' = 2\rangle$, after the MOT and the repumping beams are switched off. The $|5P_{3/2}; F' = 2\rangle$ state has a lifetime $\tau = 30\,$ns and decays both to the $|5S_{1/2}; F = 2\rangle$ and to the $|5S_{1/2}; F = 1\rangle$ states, with a branching ratio of 1/5 [12]. Although atoms in the state $|5S_{1/2}; F = 1\rangle$ are still present in the atomic cloud, they are no longer coupled to the Rydberg transition due to the large energy difference between the sub-levels of the ground state ($\approx 6,8\,$GHz). This leads to a decrease in the effective density n_{eff}, i.e, the density of atoms in the $|5S_{1/2}; F = 2\rangle$ state. In order to measure n_{eff} using this technique, after the depumping pulse goes off, we directly ionize the atoms of the cloud using the 421 nm laser and measure the number of ions created.

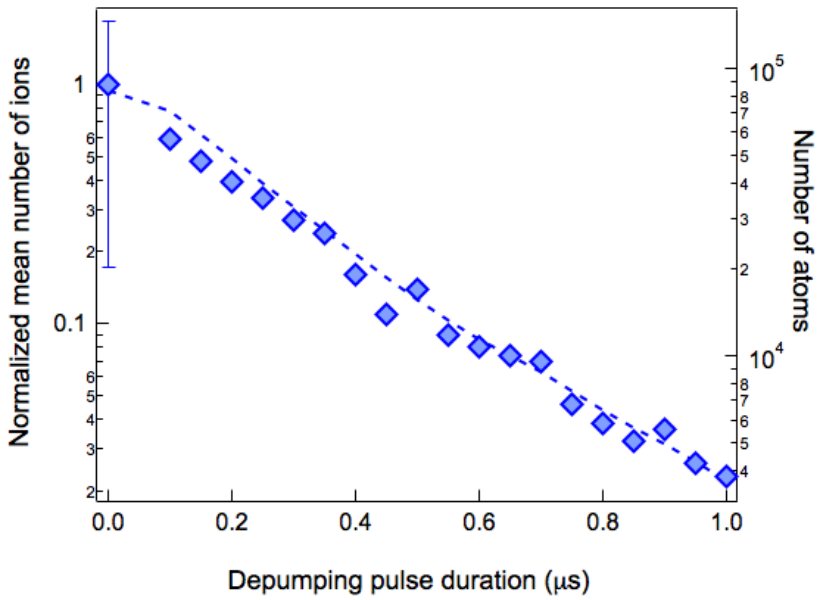

Figure 1. (Color online) Variation of the number of ions as a function of the depumping pulse duration. On the left axis, the normalized number of ions obtained as a function of the duration of the depumping pulse (blue diamonds) is plotted. The dashed line is a guide to the eye. On the right axis the number of atoms for each point is indicated.

Using this technique we managed to decrease the effective density of the sample, while its size remained constant. In Fig.1, we show data up to $1\,\mu$s of depumping pulse duration.Within this time, the effective density of the cloud decreases by 2 orders of magnitude. Increasing the

duration of the depumping pulse up to 2 μs, we were able to decrease the effective density of the sample by $3-4$ orders of magnitude, generating clouds with ≈ 10 atoms. For depumping pulse duration $> 2\,\mu$s the efficiency of this technique decreases, making it difficult to reach a regime of (on average) a single atom in the cloud.

The few atom regime could be reached using the second technique, in which we reduced the loading time (τ_{loading}) of the MOT.

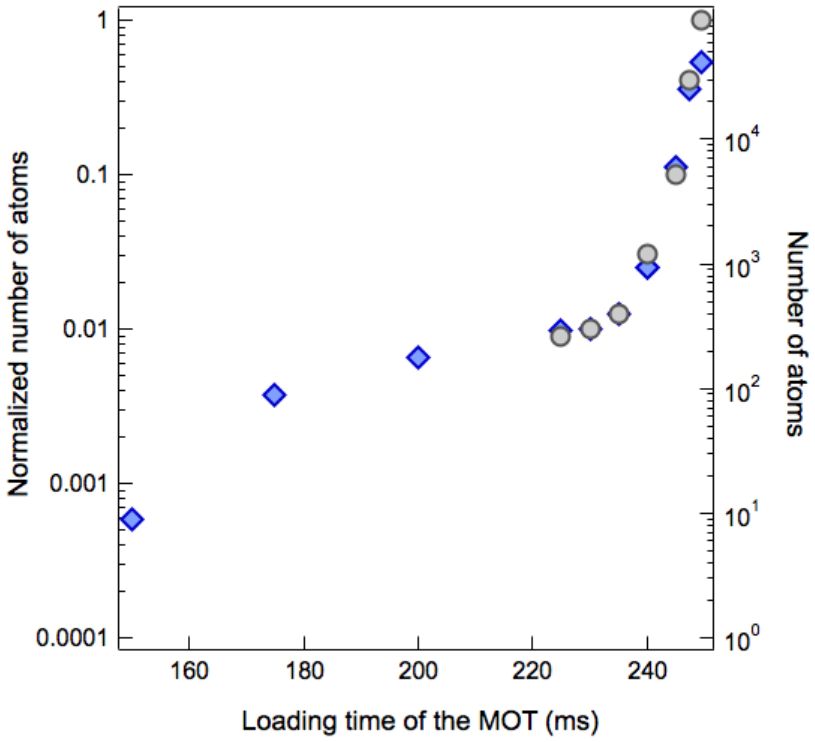

Figure 2. (Color online) Variation of the number of atoms in the MOT as a function of the loading time. On the left axis, the normalized number of atoms in the MOT is plotted as a function of τ_{loading} in ms. On the right axis it is shown the absolute value for each point. Grey circles indicate the number of atoms directly measured by the CCD camera (statistical error of $\sim 10\%$, systematic error estimated to be around a factor of 2). Blue diamonds correspond to the number of atoms calculated based on the number of ions measured when the sample is directly ionized. For both cases, the error bars are smaller than the symbols.

In Fig.2, grey circles indicate measurements of the number of atoms of the MOT taken by using a CCD camera. This device collects a portion of the light scattered by the atoms and from this signal we calculate the number of atoms in the MOT as well as its size, with a statistical error of $\sim 10\%$ (the systematic error is estimated to be around a factor of 2 due to uncertainties in the calculation of the atom number from the scattered light collected by the camera). Below $N \approx 300$ atoms, background noise made it impossible to obtain an accurate estimation of the atom number in this way. From this point (i.e., when $\tau_{\text{loading}} < 220\,$ms), N was deduced by photoionizing the sample and measuring the number of ions generated. Knowing N from CCD measurement and the number of ions created in a photoionization experiment for a certain τ_{loading}, we could extrapolate the value of N in the regime where the CCD signal measurement is not possible (blue diamonds in Fig.2). Regarding the cloud size, for τ_{loading} up to 220 μs we did not observe significant variations, which we assume to be valid also for lower values of

τ_{loading}. Hence, using this technique we were able to reach a regime with $N \leq 10$ atoms.

Both techniques offer the possibility to generate clouds from several thousands to a few atoms without changing the size of the cloud. The variation of the loading time of the MOT allows us to reach the few atom regime, whereas the depumping technique makes possible to vary the effective density of the sample at any time of the experiment.

3. Results

We now use the techniques described in the previous section to study the dynamics of Rydberg excitations in a MOT from the few atom regime up to the high density regime. The variation of the MOT τ_{loading} was used to generate single atom conditions. At $\tau_{\text{loading}} = 250\,\text{ms}$, the cloud size was $\sigma_{x,y,z} \approx 29\,\mu\text{m}$ and $N = 7.1 \cdot 10^4$, almost single atom conditions.

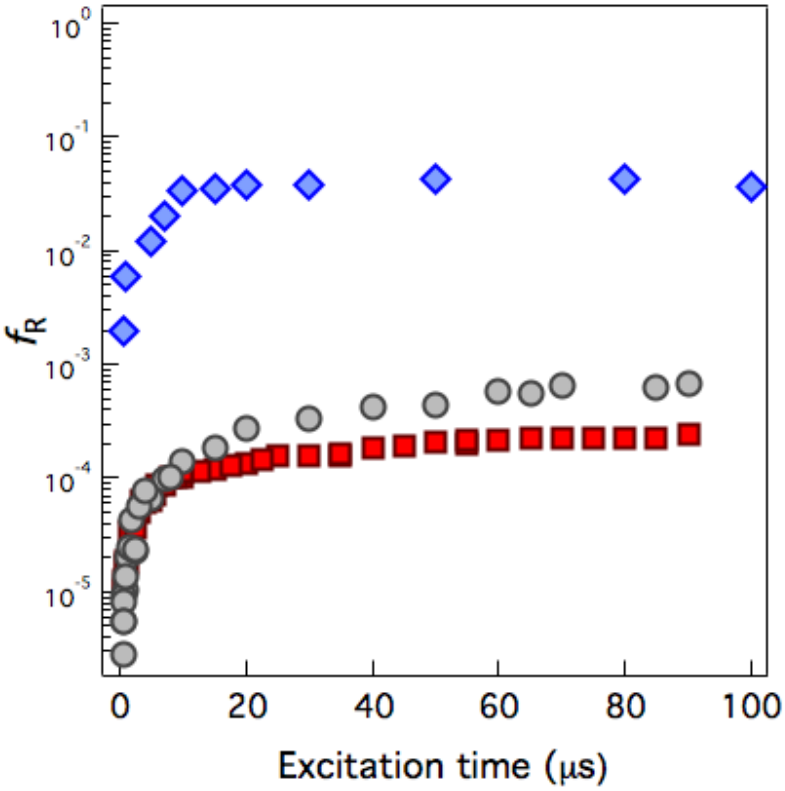

Figure 3. (Color online) Measured Rydberg fraction (f_R) as a function of the pulse duration. The densities of the different samples are: $n_{\text{eff}} \approx 6.0 \cdot 10^{10}\,\text{cm}^{-3}$ (red squares), $n_{\text{eff}} \approx 1.8 \cdot 10^{10}\,\text{cm}^{-3}$ (grey circles), $n_{\text{eff}} \approx 4.2 \cdot 10^{7}\,\text{cm}^{-3}$ (blue diamonds).

The higher effective densities were prepared using the depumping technique starting from a MOT of $n \approx 6.0 \cdot 10^{10}\,\text{cm}^{-3}$ ($\sigma_{x,y,z} \approx 160\,\mu\text{m}$, $N = 2.4 \cdot 10^5$ atoms). Because this cloud size is larger than the beams waists, only the number of atoms within the volume of interaction with the Rydberg transition lasers was considered in the calculation of the Rydberg fraction, f_R). The detuning of the intermediate state and Rabi frequencies were: $\Delta = +500\,\text{MHz}$ and $\Omega = 1.2\,\text{MHz}$, for the experiment in the few atom regime; and $\Delta = +720\,\text{MHz}$ and $\Omega = 240\,\text{kHz}$, for the high density regime experiment. In both cases, atoms were excited to the $70S$ Rydberg state, for which the blockade radius is $r_b \approx 10\,\mu\text{m}$.

In Fig.3 we show number of Rydberg excitations divided by the total number of atoms of the sample, f_R, as function of time. Red squares correspond to effective densities of:

$n_{\text{eff}} \approx 6.0{\cdot}10^{10}\,\text{cm}^{-3}$, grey circles: $n_{\text{eff}} \approx 1.8{\cdot}10^{10}\,\text{cm}^{-3}$ and blue diamonds: $n_{\text{eff}} \approx 4.2{\cdot}10^{7}\,\text{cm}^{-3}$, corresponding to interparticle distances of: $\sim 2.5\,\mu$m, $\sim 5.7\,\mu$m and $\sim 28.8\,\mu$m, respectively .

In the few atom regime, atoms oscillate between the ground and the excited state with Rabi frequency Ω. After some time, the system reaches the stationary state with a fraction of atoms in the Rydberg state $f_R = 1/2$. Taking into account our detection efficiency, $\eta \approx 50\%$, this observed fraction is expected to be $f_R = 1/4$. The measured value $f_R \approx 0.05$ (see blue diamonds in Fig.3) is significantly lower. A possible explanation can be a systematic error in the estimated number of atoms induced by systematic error in the measurement of the the CCD camera. The resolution in the atom counting could be improved either by improving the measurement technique itself, or in the subsequent image processing. In the first case, different imaging techniques, ranging from the use of beams of high intensity to maximize the photon scattering rate [13] to the reduction of the energy released in light-assisted collisions between atoms [14] could be implemented; whereas an advanced postprocessing of the images through the combination of a fringe removal algorithm and maximum likelihood estimation[15] provides also an enhanced sensitivity on the readout of the atom number.

Another possible source of error could be that the expected f_R considers that all the atoms are driven with the same Rabi frequency and thus, reach the stationary state at the same time, which is clearly not the case for the gaussian intensity distribution of the excitation lasers of our experiment.

In the higher density regimes, f_R is much lower than in the few atom case because the number of atoms able to be excited to the Rydberg state is much smaller than the number of atoms in the ground state. This happens mainly due to the effect of dipole blockade [16], i.e., a suppression of excitation of an atom by an already excited one within the blockade sphere [17–19]. Alternatively, this effect can be interpreted as a manifestation of kinetic constraints that slow down the dynamics [9].

4. Conclusion

In conclusion we have presented two different experimental techniques to prepare atomic samples of different density regimes. Both of them offer the possibility to generate clouds from several thousands to few atoms. This could be applied to explore the behavior of Rydberg samples in an incoherent driving scenario, where kinetic constraints are expected to become manifest. Additionally, the depumping technique allows us to vary the density of the sample at any time of the experiment which permits us to, e.g., generate Rydberg atoms in a high density regime and, after some time, to remove the ground state atoms from the cloud.

Acknowledgments

We acknowledge financial support from the EU Marie Curie ITN COHERENCE Network.

References

[1] Gallagher T F 1994 *Rydberg Atoms* (Cambridge University Press)

[2] Gallagher T F and Pillet P 2008 *Advances In Atomic, Molecular, and Optical Physics* **56** 161 – 218

[3] Jaksch D, Cirac J I, Zoller P, Rolston S L, Côté R and Lukin M D 2000 *Phys. Rev. Lett.* **85** 2208

[4] Lukin M D, Fleischhauer M, Côté R, Duan L M, Jaksch D, Cirac J I and Zoller P 2001 *Phys. Rev. Lett.* **87** 037901

[5] Urban E, Johnson T A, Henage T, Isenhower L, Yavuz D D, Walker T G and Saffman M 2009 *Nat. Phys.* **5** 110

[6] Gaëtan A, Miroshnychenko Y, Wilk T, Chotia A, Viteau M, Comparat D, Pillet P, Browaeys A and Grangier P 2009 *Nat. Phys.* **5** 115

[7] Dudin Y O, Li L, Bariani F and Kuzmich A 2012 *Nat. Phys.* **8** 790

[8] Gärttner M, Whitlock S, Schönleber D and Evers J 2014 *eprint arXiv:1408.2453*

[9] Lesanovsky I and Garrahan J P 2013 *Phys. Rev. Lett.* **111**(21) 215305

[10] Viteau M, Radogostowicz J, Chotia A, Bason M G, Malossi N, Fuso F, Ciampini D, Morsch O, Ryabtsev I and Arimondo E 2010 *J. Phys. B: At. Mol. Opt. Phys.* **43** 155301

[11] Valado M M, Malossi N, Scotto S, Ciampini D, Arimondo E and Morsch O 2013 *Phys. Rev. A* **88**(4) 045401

[12] Steck D A URL `http://steck.us/alkalidata/rubidium87numbers.pdf`

[13] Muessel W, Strobel H, Joos M, Nicklas E, Stroescu I, Tomkovič J, Hume D and Oberthaler M 2013 *Applied Physics B* **113** 69

[14] McGovern M, Hilliard A J, Grünzweig T and Andersen M F 2011 *Opt. Lett.* **36** 1041

[15] Ockeloen C F, Tauschinsky A F, Spreeuw R J C and Whitlock S 2010 *Phys. Rev. A* **82** 061606

[16] Comparat D and Pillet P 2010 *J. Opt. Soc. Am. B* **27** A208

[17] Vogt T, Viteau M, Chotia A, Zhao J, Comparat D and Pillet P 2007 *Phys. Rev. Lett.* **99** 073002

[18] Tong D, Farooqi S M, Stanojevic J, Krishnan S, Zhang Y P, Côté R, Eyler E E and Gould P L 2004 *Phys. Rev. Lett.* **93** 063001

[19] Singer K, Reetz-Lamour M, Amthor T, Marcassa L G and Weidemüller M 2004 *Phys. Rev. Lett.* **93** 163001